ACS APPLIED BIO MATERIALS

www.acsabm.org Article

Gold Nanoparticle-Assisted CRISPR-Cas12a-Based Activity Assay for Highly Sensitive Detection of Trypsin

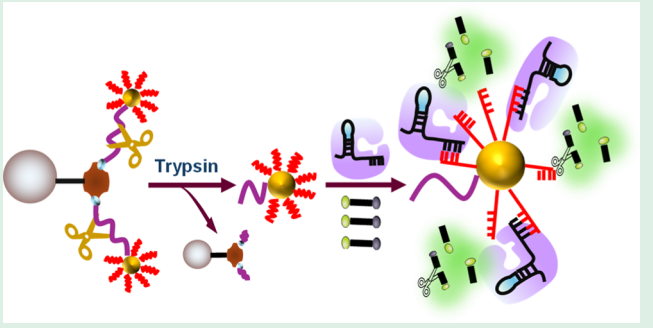
Sathishkumar Munusamy, Haiyan Zheng, Jun Chen, Shuo Zhou, Juanhua Kong, Rana Jahani, Yuan Zhao, and Xiyun Guan*

Cite This: https://doi.org/10.1021/acsabm.5c00854 Read Online

ACCESS | Metrics & More | Article Recommendations | Supporting Information

Downloaded via SHANGHAI NORMAL UNIV on June 18, 2025 at 01:58:49 (UTC).
See https://pubs.acs.org/sharingguidelines for options on how to legitimately share published articles.

ABSTRACT: Proteases play important roles in diverse physiological processes, and their malfunction has been implicated in various conditions and diseases. Therefore, development of sensitive methods for protease detection in clinical samples is highly desired for disease diagnosis. Herein, we report an ultrasensitive and selective CRISPR-Cas12a based fluorescent assay for trypsin activity measurement. By taking advantage of the signal amplification brought by a unique magnetic bead-gold nanoparticle assembly, which carries the peptide substrate and tens to hundreds of DNA molecules per peptide molecule, trypsin can be detected with a limit of detection reaching as low as 0.13 ng/mL. Furthermore, the sensor selectivity study was performed by examining several biomolecules commonly present in biological samples, including bovine serum albumin (BSA), human serum albumin (HSA), DNase, RNase, chymotrypsin, elastase, and thrombin. Moreover, trypsin inhibition and serum sample analysis were successfully carried out. Given the ultrahigh sensitivity, the CRISPR-based trypsin activity assay developed in this work can be used as a generic platform for developing sensors for other proteases, offering the potential as a noninvasive/minimally invasive tool for clinical diagnosis.



KEYWORDS: *proteases, gold nanoparticles, peptides, DNA, CRISPR, fluorescence*

INTRODUCTION

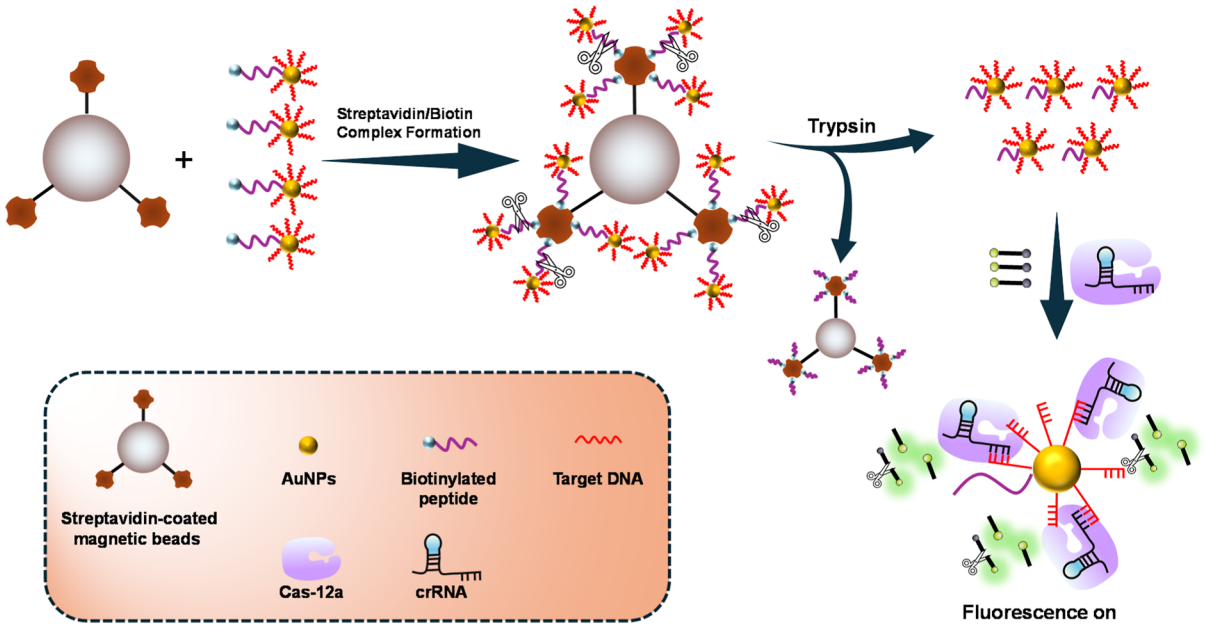
Proteases are essential regulators of diverse physiological processes, and their malfunction has been implicated in various conditions and diseases such as inflammation, viral infections, cancer, and neurodegenerative diseases.[1−4] As one specific example, trypsin is a pancreatic serine protease with a molecular weight of 23.8 kDa that cleaves proteins and peptides at the carboxyl side of lysine and arginine residues and hence it is crucial for digestion.[5,6] Apart from its digestive function, trypsin plays a critical role in the regulation of the activities of other proteins, and disturbed activity of trypsin is strongly implicated in pancreatitis and pancreatic cancer.[7,8] In healthy individuals, normal urinary trypsin levels range between 115 and 350 ng/mL, while the trypsin concentration can go up to as high as 84.4 μg/mL in acute cases of pancreatitis.[9,10] Therefore, trypsin is an important biomarker for pancreatic health, and development of sensitive methods for detection of trypsin in clinical samples is highly desired for diagnosis of pancreatic and chronic systemic diseases. Thus, far, many methods have been reported for trypsin detection, including the mass spectrometry,[11] enzyme-linked immunosorbent assay (ELISA),[12] gel electrophoresis,[13] electrochemical analysis,[14−17] chemiluminescence spectrometry,[18] nanopore sensing,[19] colorimetric spectrometry,[20] and fluorescence spectrometry.[21−24] Among them, fluorescence spectroscopy has gained a lot of attention because of some of its unique advantages such as low background noise, high sensitivity, and easy operation. However, the current existing fluorescence-based trypsin assays are still plagued with several problems, such as the toxicity of quantum dots, the low sensitivity of "turn-off" detection, and the requirement of numerous reagents.

Gold nanoparticles (AuNPs) have been extensively used in biological applications, owing to their size- and shape-dependent optical and electronic properties.[25−31] Various AuNP-based trypsin assays have been reported, most of which are based on the aggregation or deaggregation of peptide-functionalized AuNPs to produce a colorimetric signal.[32−35] In addition to these aggregation-based approaches, growth-mediated AuNP sensors have also been developed. As a noted example, Creyar et al. constructed a peptide-gold

Received: May 6, 2025
Revised: June 11, 2025
Accepted: June 12, 2025

© XXXX American Chemical Society

Scheme 1. Schematic Representation of the Key Procedure of Synthesizing the Magnetic Bead-Gold Nanoparticle Assembly and the Principle of the CRISPR-Based Trypsin Activity Assay (Not to Scale)



nanoparticle system that leveraged the differential adsorption of a parent peptide and its cleaved counterpart to control the growth of gold nanorods in response to trypsin exposure.[36] With the dithiol peptide GCKGCG, they showed that cleavage of the peptide yielded a dispersion of high-aspect-ratio rods, low-aspect-ratio rods, and faceted nanospheres. The subsequent particle morphology alterations were efficient in the modulation of solution optical properties and were directly proportional to enzyme activity. Despite the significant advancements in nanotechnology, most of the nanomaterial-based trypsin sensing methods suffer from poor limits of detection and involve time-consuming AuNP-peptide substrate preparation procedures. In this work, we are demonstrating a fundamentally different new strategy for ultrasensitive trypsin activity assay by taking advantage of dual-functionalized AuNPs-assisted signal amplification, where each trypsin-peptide substrate cleavage event is converted to numerous barcode DNA molecules with predesigned sequences, followed by CRISPR-Cas12a-based fluorescence analysis. While traditionally used for nucleic acid analysis, CRISPR-Cas12a systems can also be adapted to detect various non-nucleic acids.[37−40] Our developed sensing strategy can be used as a generic method for developing sensors for other proteases, thus offering a potential use as a noninvasive/minimally invasive tool in clinical diagnosis.

EXPERIMENTAL SECTION

Materials and Reagents. Streptavidin-coated magnetic beads (2.8 μm diameter, 10 mg/mL) were obtained from Invitrogen (Carlsbad, CA, USA), while a 30 nm-diameter gold colloidal solution was procured from Nanopartz (Loveland, CO, USA). LbCas12a and all the DNA/RNA samples were ordered from Integrated DNA Technologies (Coraville, IA, USA). The peptide used in this work was synthesized using the AAPPTEC 396 omega peptide synthesizer at the Molecular Interactions Core of the University of Missouri (Columbia, MO). All the other chemicals, including trypsin, RNase A, DNase A, BSA, HSA, chymotrypsin, elastase, thrombin, and so on were purchased from Sigma-Aldrich (St. Louis, MO).

Preparation of Dual Functionalized AuNPs. The dual functionalized AuNPs were synthesized via a two-step process. First, a biotinylated peptide (sequence: Biotin-Lys-Lys-Lys-Ly-Tyr-Lys-Lys-Lys-Ly-Tyr-Lys-Lys-Lys-Ly-Tyr-Lys-Lys-Lys-Ly-Tyr-Cys) was conjugated to AuNPs of 30 nm diameter via the Au−S bond according to a procedure as described in detail elsewhere.[41−43] Briefly, 100 μL of colloidal AuNPs (3 μM) was first combined with 5 μL of 2 M NaOH with gentle mixing. Then, the biotinylated peptide solution (2.5 μL, 100 μg/mL) was added, and the mixture was gently mixed again and vortexed at room temperature for 30 min, resulting in the formation of peptide-modified AuNPs (Pep-AuNPs). During the second step, ssDNA was immobilized to Pep-AuNPs. For this purpose, a 100 μL of 20-mer disulfide-terminated ssDNA (TD, sequence: 5′−HS−S−$(CH_2)_6$−TTTTTTTTTTTTTTTTTTTT-3′, 1 mM) was first incubated with TCEP (tris(2-carboxyethyl)phosphine) at ambient temperature for 1 h, thereby reducing the disulfide linkage and releasing free thiol groups. The thiol-terminated ssDNA (100 μL) was then combined with peptide-AuNPs and gently mixed for 1 h at room temperature to facilitate DNA binding. After that, an "aging-salting" step[42] was carried out by gradually increasing the NaCl concentration to 0.3 M using a 2 M NaCl solution, and the mixture was left overnight to enhance DNA loading. Finally, the solution was centrifuged at 10,000g for 10 min to remove any unbound moieties, yielding purified, ssDNA-decorated nanoparticles (Pep-AuNPs-TD).

Formation of MB−AuNPs Assembly. Streptavidin-functionalized magnetic beads (MBs) (10 μL) were washed three times with 500 μL of washing buffer, consisting of 10 mM PBS (pH 7.2) and 0.1% BSA. After the final wash, the beads were resuspended in 500 μL of PBS (pH 7.2). Then, 5 μL of dual functionalized AuNPs (Pep-AuNPs-TD) were introduced into the suspension, followed by vortexing and stirring for approximately 30 min to facilitate binding. After incubation, unbound nanoparticles were removed by washing the functionalized magnetic beads three times with 10 mM PBS (pH 7.2) containing 0.1% Tween. The prepared MB-Pep-AuNPs-TD complex served as a substrate for the trypsin cleavage.

Procedure for the CRISPR-Based Trypsin Assay. The prepared MB-Pep-AuNPs-TD complex was resuspended in 1 mL of 10 mM PBS (pH 7.2) with 0.1% Tween. Trypsin, at a concentration ranging from 1 to 100 ng/mL, was added to the suspension, and the mixture was vortexed and stirred at room temperature for 20 min. After the reaction, the magnetic beads were separated, and the solution devoid of magnetic beads was collected for CRISPR analysis using a protocol

https://doi.org/10.1021/acsabm.5c00854
ACS Appl. Bio Mater. XXXX, XXX, XXX−XXX

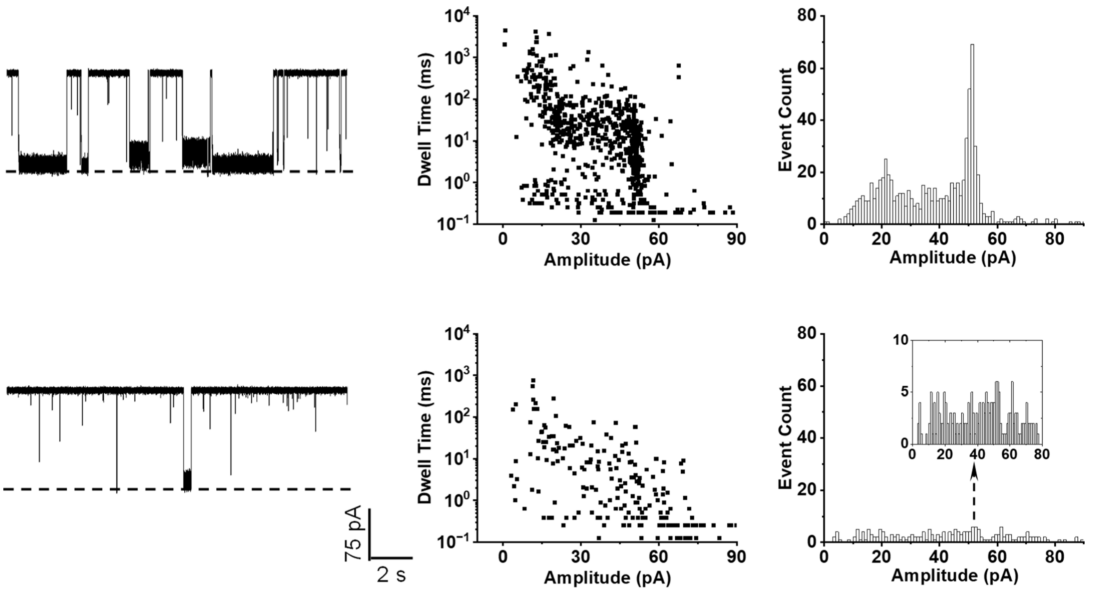


Figure 1. Nanopore analysis of trypsin-peptide substrate cleavage interaction. (Top Panel) Without and (Bottom Panel) with trypsin. (Left) Typical single-channel current recording trace segments; (middle) the corresponding scatter plots of event amplitude versus residence time; and (right) the event-list histograms. The experiment was carried out at +150 mV in an electrolyte solution containing 1 M NaCl and 10 mM Tris (pH 7.5) and in the presence of 5 μM of peptide. The $(M117F)_7$ α-hemolysin protein was used as the nanopore sensing element, which was added to the grounded *cis* chamber compartment. In the experiment showing in the bottom panel, nanopore single-channel recording was carried out after incubating the peptide-trypsin mixture in the 1 M NaCl electrolyte solution for 6 min. The peptide or peptide-trypsin mixture was added to the *trans* compartment. Scatter plots and event-list histograms were obtained based on 7 min trace segments. Trypsin concentration was 1000 ng/mL.

as described in a previous work.[41] Briefly, a mixture containing 4 μL of Cas12a (1 μM), 6 μL of crRNA (sequence: rUrArArUrUrUrCrUrArCrUrArArGrUrGrUrArGrArUrArArArArArArArArArArArArArArArA, 2 μM), and 20 μL of 1× NEB Buffer 3.1 was incubated at room temperature for 30 min to facilitate Cas12a-crRNA complex formation. Subsequently, the collected supernatant (1 mL) was introduced into the preformed Cas12a-crRNA complex and allowed to react for an additional 30 min at room temperature. Following this, a dye-labeled single-stranded DNA (ssDNA, sequence: FAM-TTATT-IABkFQ) reporter substrate (10 μL, 5 μM) was added to the reaction mixture and incubated for 3 h. The fluorescence signal was then measured at an excitation/emission wavelength of 492/528 nm at room temperature.

RESULTS AND DISCUSSION

The Principle of the CRISPR-Based Trypsin Activity Assay. Unlike the traditional protease activity assay, which is carried out by directly monitoring the cleavage of a highly selective dye-labeled peptide substrate by the target protease via the change in the colorimetric or fluorescent signal, the trypsin activity assay developed in this work takes advantage of a unique magnetic bead-gold nanoparticle assembly (Scheme 1), which carries the peptide substrate and multiple (tens to hundreds of) DNA molecules per peptide molecule. Upon exposure to trypsin, it will cleave the peptide which connects the gold nanoparticles (AuNPs) and streptavidin-functionalized magnetic beads (MBs), thus liberating DNA-carrying AuNPs into the solution. The DNA molecules immobilized on the surface of AuNPs then activate the CRISPR-Cas12a system via specific recognition by the Cas12a-crRNA complex, initiating its characteristic collateral cleavage activity, thus breaking down the dye-labeled reporter ssDNA, producing fluorescence. In contrast, if the sample does not contain trypsin, the magnetic bead-gold nanoparticle assembly will be intact, and no DNA-carrying AuNPs will be released, leading to no fluorescence signal being detected. It is worth mentioning that, in our design, since each peptide-trypsin cleavage event yields numerous DNA molecules for downstream CRISPR analysis, our developed protease activity assay platform offers an enhanced sensitivity than the traditional protease assays.

Design of Peptide Substrate for Trypsin Cleavage. Trypsin, a serine protease with 223 amino acid residues, is the most important digestive enzyme produced in the pancreas, which cleaves peptide bonds mainly at the carboxyl side of the lysine or arginine amino acid residue. Since acute pancreatitis patients have significantly elevated trypsin levels in their sera, trypsin is a useful biomarker for pancreatitis. To develop a highly sensitive assay for trypsin, we designed a 21-mer biotinylated peptide mainly consisting of lysine amino acids (sequence: Biotin-KKKKYKKKKYKKKKYKKKKYC). Note that, trypsin has a dimension of 3.8 nm × 3.8 nm × 3.8 nm,[44] while the estimated length of the 21-mer peptide is ~8.4 nm (based on an average contour length per amino acid of 4.0 Å). Therefore, we expect that trypsin can access and interact with the cleavage site of the peptide substrate even after the biotin moiety of the peptide is conjugated to the streptavidin-modified MBs, while its C-terminal cysteine is coupled to the surface of AuNPs. To verify the feasibility of using our designed biotinylated peptide as an effective substrate for trypsin cleavage, the peptide-trypsin interaction was first investigated using the $(M117F)_7$ α-hemolysin nanopore using a procedure described previously.[45] Nanopore stochastic sensing is an emerging single-molecule detection technique. By monitoring ionic current modulations caused by passage of molecular or ionic species through a single nanoscale-sized pore in a high salt solution, it has been utilized as a versatile tool to explore a wide variety of applications, including investigation of enzyme kinetics and thermodynamics.[46−51] We found that, in the absence of trypsin, the peptide produced two major types of events in the nanopore: one type having a mean

https://doi.org/10.1021/acsabm.5c00854
ACS Appl. Bio Mater. XXXX, XXX, XXX−XXX

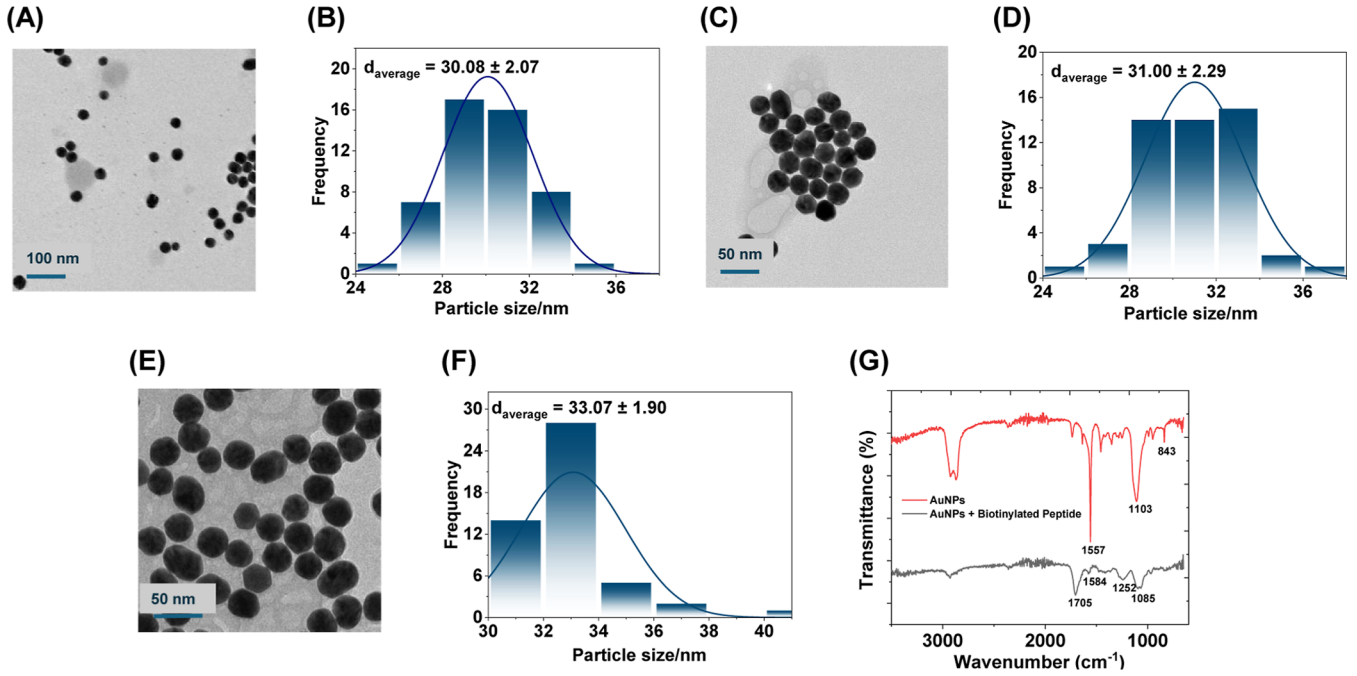


Figure 2. Characterization of dual functionalized AuNPs. (A) Representative TEM image and (B) size distribution of citrate-capped AuNPs; (C) representative TEM image and (D) size distribution of peptide-functionalized AuNPs (Pep-AuNPs); (E) representative TEM image and (F) size distribution of peptide-functionalized AuNPs after further conjugation with ssDNA (Pep-AuNPs-TD); and (G) FT-IR spectrum of AuNPs and Pep-AuNPs. TEM was performed using a JEOL JEM-1400 instrument at 120 kV, while IR spectra were acquired on an FTIR PerkinElmer Spectrum Two: UATR Two spectrometer using 1 cm^{-1} resolution.

residual current of 21.5 ± 0.7 pA and a long-lived residence time of 42.8 ± 3.9 ms, while the other showing a residual current of 51.0 ± 0.1 pA and a smaller residence time of 6.20 ± 0.87 ms. These events might be attributed to the different orientations in which the peptide entered and passed through the nanopore although we could not rule out the possibility that they were due to the biomolecules' translocation and collision with the nanopore, as reported in the previous work.[52] In contrast, upon addition of trypsin to the peptide, the frequency of these peptide current modulation events decreased significantly (Figure 1), indicating the successful cleavage of the peptide by trypsin. Therefore, the experimental results confirmed that the peptide we designed was an appropriate substrate for trypsin activity assay at the molecular level.

Characterization of Dual Functionalized AuNPs. One of the major components for our pioneered CRISPR-based trypsin activity assay is the dual functionalized AuNPs. To verify the successful synthesis of peptide/DNA-dual functionalized AuNPs, UV−vis absorption spectroscopy, transmission electron microscopy (TEM), and infrared (IR) spectroscopy experiments were performed, with the results summarized in Figure 2. Briefly, UV−vis experiments showed a significant red shift of the surface plasmon resonance (SPR) peak from ∼521 nm (pure AuNPs, red curve) to ∼ 523 nm (peptide-functionalized AuNPs, black curve), along with a decrease in the absorption intensity (Supporting Information, Figure S1). On the other hand, TEM characterization gave in-depth understanding of morphological changes between the free and functionalized AuNPs. For example, unmodified AuNPs displayed mostly spherical shapes with even distribution (Figure 2A), with a mean particle size of 30.08 ± 2.07 nm (Figure 2B). After immobilizing peptide molecules to AuNPs, there was a detectable increase in the particle size by about 1 nm relative to the unmodified nanoparticles (Figure 2C,D). Further coupling DNA to the peptide-modified AuNPs led to another increase in the particle size (by 2 nm) to 33.07 nm (Figure 2E,F). This size augmentation provides compelling evidence of the successful and sequential functionalization of AuNPs with both the peptide and DNA. In addition, the FT-IR spectrum (Figure 2G) of the unmodified AuNPs exhibits a distinct peak at 843 cm^{-1}, corresponding to the metal−oxygen stretching vibration, confirming the coordination of citrate ions to the gold nanoparticle surface via $RCOO^- \rightarrow Au$ interaction. Further confirmation of citrate capping on AuNPs was provided by peaks at 1557 cm^{-1} and 1103 cm^{-1}, assignable to the R−CO_2 and C−O stretching vibrations, respectively. In contrast, after attaching the peptide to AuNPs, the Pep-AuNPs sample showed obvious spectral shifts (the peaks appearing at 1584 cm^{-1} and 1085 cm^{-1}), which indicates the successful coordination of the ligands onto the surface of nanoparticles. Furthermore, the existence of an Amide I band close to 1705 cm^{-1} (due to the C═O stretching of the peptide bonds) provides another evidence for the conjugation of the peptide molecules on AuNPs. Moreover, the peak at 1252 cm^{-1}, which is attributed to C−N−C stretching of the peptide backbone, further confirms the successful attachment of the peptide on the surface of the nanoparticles. Taken together, the combined UV−vis, TEM and IR experimental results confirm that the AuNPs were indeed effectively modified with both the peptide and DNA.

OPTIMIZATION OF THE EXPERIMENTAL CONDITIONS

It should be noted that, in our sensing design, the molar ratio of the DNA to peptide molecules immobilized on the AuNPs surface is critical to the sensor sensitivity since each peptide-trypsin cleavage event yields multiple (tens to hundreds of) DNA molecules for

https://doi.org/10.1021/acsabm.5c00854
ACS Appl. Bio Mater. XXXX, XXX, XXX−XXX

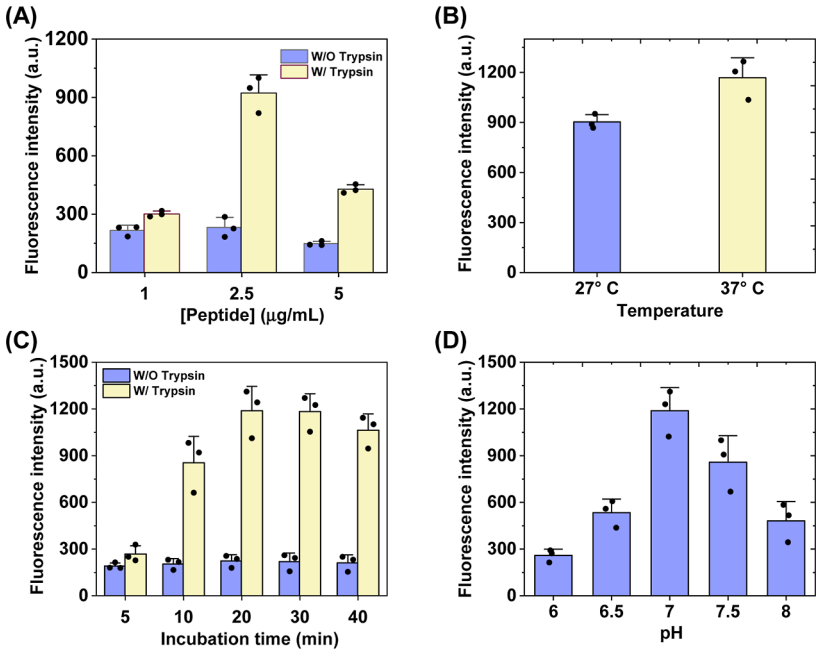


Figure 3. Effect of (A) the loading density of the biotinylated peptide on the surface of dual-functionalized AuNPs; (B) temperature; (C) incubation time; and (D) solution pH on trypsin detection. Fluorescence measurements were recorded at λex/em = 492/528 nm at room temperature. The concentration of trypsin used in Figure 3 was 100 ng/mL. Each data point represents the mean ± standard deviation from three independent replicates.

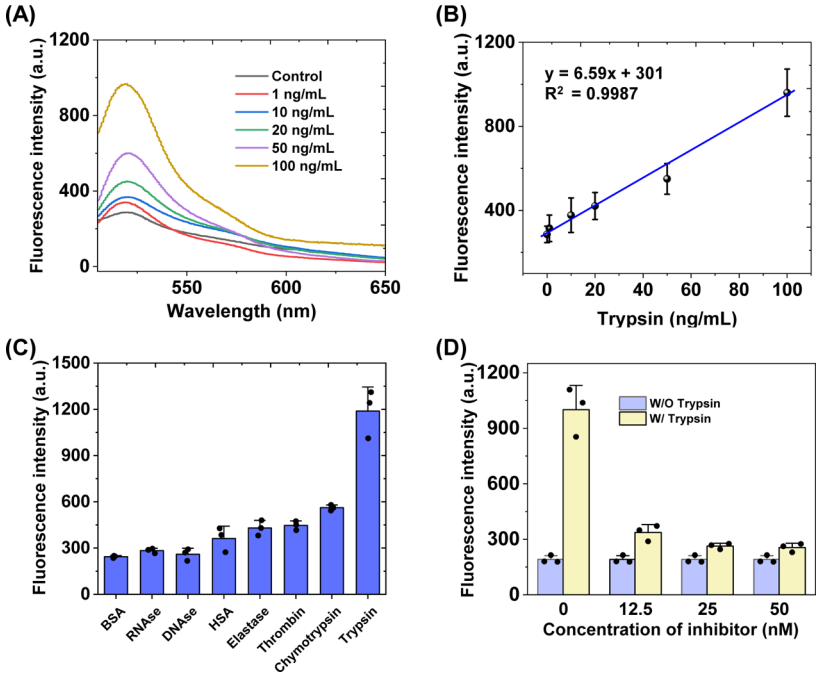


Figure 4. Performance of the trypsin sensor. (A) Fluorescence emission spectra, illustrating the variation in the fluorescence intensity as a function of increasing trypsin concentration; (B) the corresponding dose−response curve, showing the linear relationship between the fluorescence intensity at 525 nm and trypsin concentration; (C) selectivity study; and (D) trypsin inhibition investigation. Except trypsin, the concentrations of all the other biomolecular species used in Figure 4C were 1000 ng/mL each. In Figure 4D, the mixture solutions of trypsin (100 ng/mL) and its inhibitor with concentrations ranging from 12.5 to 50 nM were incubated at room temperature for 10 min before analyzed by the trypsin sensing platform. Data represent the mean ± standard deviation from three independent replicates.

downstream CRISPR analysis. In principle, a larger molar ratio of DNA to peptide leads to a decrease in the limit of detection (LOD) of the sensor, which has been demonstrated in our earlier studies,[42] where antibody/DNA-dual functionalized AuNPs were used to detect proteins. However, a too low peptide density on AuNPs might lead to a consequence that the crowdy DNA molecules surrounding the peptide substrate prevent it being accessible by the target trypsin, thus having a negative impact on the sensor sensitivity. To achieve highly sensitive detection of trypsin, a series of dual functionalized AuNPs having varying peptide loading densities was prepared by incubation of AuNPs (30 nm diameter, 3 μM) with biotinylated peptides at different concentrations (ranging from 1 to 5 μg/mL in Figure 3) and

https://doi.org/10.1021/acsabm.5c00854
ACS Appl. Bio Mater. XXXX, XXX, XXX−XXX

a fixed concentration of DNA (10 μM). These functionalized AuNPs with different peptide loading densities were then coupled to streptavidin-functionalized MBs, followed by digestion by trypsin (100 ng/mL) and CRISPR analysis. We found that the functionalized AuNPs prepared with 2.5 μg/mL of peptide yielded the largest fluorescent intensity, followed by AuNPs functionalized with 5 μg/mL of peptide (Figure 3A). The AuNPs modified with 1 μg/mL of peptide showed a very small signal-to-noise ratio (1.30), indicating the strong steric hindrance effect of the surrounding DNA on peptide/trypsin cleavage.

Using the MB−AuNPs assembly (i.e., the MB-Pep-AuNPs-TD complex) prepared with 2.5 μg/mL of peptide, several parameters that are key to the enzymatic reactions were then systematically investigated, including incubation time and temperature as well as solution pH. We found that, when the temperature increased from 27 to 37 °C, a slight (24.6%) increase in the fluorescence intensity was observed (Figure 3B), suggesting that temperature was not a critical factor in our sensor system. In contrast, with an increase in the incubation time, the fluorescence signal increased significantly and reached its maximum when the incubation time was 20 min (Figure 3C). Hence, 20 min was selected as the optimum incubation time and used in the subsequent experiments. Moreover, the pH experiments showed that the optimal pH for maximum trypsin activity was 7.5, and a decease or an increase in the solution pH resulted in smaller fluorescence signals (Figure 3D).

Performance of the Trypsin Sensor and Trypsin Inhibition Investigation. Under the optimized dual functionalized AuNPs, solution pH, and incubation time and temperature, as well as the CRISPR analysis system containing Cas12a, crRNA and ssDNA reporter in 1:3:12.5 molar ratio, the CRISPR-based trypsin activity assay platform was used to analyze a series of trypsin solutions with varying concentrations ranging from 1 to 100 ng/mL. The experimental results revealed a consistent and noticeable increase in the fluorescence intensity at 525 nm as the trypsin concentration increased (Figure 4A). By plotting the fluorescence intensity at 525 nm against the trypsin concentration, a linear relationship with R^2 = 0.9987 was established within the concentration range of 1−100 ng/mL (Figure 4B). The limit of detection (LOD) was determined to be 0.3 ng/mL using the formula of LOD = 3σ/S.[53,54] To our best knowledge, such a LOD is much better than other nanomaterial-based detection methods developed thus far (Supporting Information, Table S1). For example, the LODs for trypsin detection by using aggregation−deaggregation-triggered fluorescent chemosensors range from 6.41 to 37.1 ng/mL,[10,23,55] while detection strategies based on optical property changes (prompted by variations in the aggregation or clustering of nanomaterials following trypsin treatment) usually detect trypsin with LODs reaching 0.045 μg/mL to 2.96 mg/mL.[20,56] Since the serum trypsin concentration in the healthy population ranges from 115 to 350 ng/mL, our method is more than good enough for clinical sample analysis. To determine the sensor selectivity, several biomolecules commonly present in biological samples were selected as potential interfering species, including BSA, HSA, DNase, RNase, chymotrypsin, elastase, and thrombin. These biomolecules were analyzed by our sensor with concentrations 10-fold higher than that of trypsin. As illustrated in Figure 4C, the fluorescence signals generated by these samples were ∼2 to 5 times smaller than the target analyte, demonstrating that the sensor was highly selective to trypsin. It should be noted that, among all the potential interfering species investigated, chymotrypsin produced the largest fluorescence intensity. The results are not unreasonable considering that chymotrypsin can also cleave this peptide substrate which contained tyrosine residues. If reducing the signal generated by chymotrypsin is desired, a new peptide sequence which does not contain aromatic residues could be used. Moreover, in real-world application, endogenous nucleic acids and DNases present in the sample might potentially interfere with our developed trypsin sensor if the nucleic acids contained the same sequence segment as our designed barcode DNA or the DNase concentration was high (several orders of magnitude larger than trypsin). In the former, the endogenous nucleic acids would activate Cas12a, while in the latter, DNases might degrade the barcode DNA and dye-labeled ssDNA reporter. If that is the case, nucleic acids can be separated from the clinical sample by extraction or be degraded by using nucleases such as DNases, while DNases can be eliminated by using DNase removal reagents.

It should be noted that proteases play key roles in diverse biological processes. Accordingly, alterations in their structure and expression patterns underlie many human pathological processes. Hence, proteases are important targets for drug discovery, and numerous protease inhibitors have been identified and widely used to treat various human diseases by suppressing protease activity via the formation of stable complexes through hydrogen bonding at the enzyme's active center, thus effectively blocking its functionality. To show our developed trypsin sensing platform can be used as a convenient tool to investigate protease inhibition, the inhibitory efficacy of a commercially available trypsin inhibitor against trypsin was investigated. We found that in the absence of the inhibitor, the trypsin sample (100 ng/mL) yielded a high fluorescence signal compared with the blank control. In contrast, when a preincubated mixture of trypsin and its inhibitor was introduced to the sensing system, a significant decrease in the fluorescence intensity was observed (Figure 4D). Moreover, with an increase in the concentration of added trypsin inhibitor, the trypsin-inhibitor mixture sample showed a decreased fluorescence signal. Therefore, the results unequivocally demonstrates that the trypsin inhibitor can indeed effectively block the trypsin activity.

Improvising the Sensitivity of the Trypsin Assay. In our trypsin sensor design outlined in Scheme 1, the CRISPR system was utilized to directly analyze the target DNA immobilized on the surface of AuNPs. It is likely that the steric hindrance of the crowded AuNPs surface might affect the binding between the Cas12a-crRNA complex and DNA, thus influencing the sensor sensitivity. To improve the LOD of the trypsin sensor, we attempted a strategy to enhance the accessibility of the target DNA by releasing it from the surface of AuNPs by using dithiothreitol (DTT). DTT, a well-characterized reducing agent, exhibits a strong affinity for the AuNPs surface due to its thiol groups, which readily form thiol-gold bonds. When an excess amount of DTT is added to DNA-functionalized AuNPs (via Au−S bond formation), it would displace the target DNA from the AuNPs, thus effectively transferring it into the solution, where it would be fully accessible for the subsequent CRISPR assay. For this purpose, after the trypsin digestion step, the product obtained was treated with 10 μL of 15 mM DTT for 10 min, followed by CRISPR analysis. The experimental results showed that, using this strategy, the LOD of the trypsin sensor could be improved to 0.2 ng/mL (Figures 5 and S2). It should be noted that, an appropriate concentration of DTT used for recovery of the target DNA was critical to the improvement in the sensor LOD. In general, with an increase in the DTT concentration, the background fluorescence intensity increased, leading to a decrease

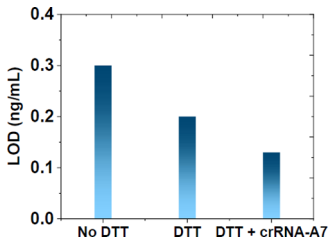


Figure 5. Effect of DTT and guide RNA on the LOD of the trypsin sensor. The experiments were performed by using a CRISPR system containing Cas12a, crRNA and ssDNA reporter in 1:3:12.5 molar ratio to analyze the digestion product of MB-Pep-AuNPs-TD by trypsin without/with DTT treatment, and employing a CRISPR system containing Cas12a, crRNA-A7 and ssDNA reporter in 1:3:12.5 molar ratio to analyze the digestion product of MB-Pep-AuNPs-TD by trypsin coupled with DTT treatment, respectively.

https://doi.org/10.1021/acsabm.5c00854
ACS Appl. Bio Mater. XXXX, XXX, XXX−XXX

in the signal-to-noise ratio, and hence a poorer sensor performance would occur.

Moreover, Cas12a crRNAs are typically 42 nucleotides (nt) long, and can be divided into two regions: a 20 nt stem-loop region and a 20−24 nt target-specific region. Previous studies have reported that engineered crRNAs with 3′- or 5′-end extensions of single-stranded nucleic acid could significantly enhance the CRISPR-Cas12a activity by increasing collateral cleavage efficiency.[57] Among them, a 7-mer extension has been identified as a universal and spacer-independent enhancer which can significantly improve both the sensitivity and specificity of LbCas12a-based nucleic acid detection. Building on this finding, a 7-mer extended guide RNA (crRNA-A7, sequence: rUrArArUrUrUrCrUrArCrUrArArGrUrGrUrArGrArUrArArArArArArArArArArArArArArArArArArATATTATT) was employed instead of the crRNA having a regular length in the CRSPR analysis system; furthermore, the collected product after trypsin digestion was treated with DTT before CRISPR analysis. As anticipated, this strategy could further improve the sensor sensitivity, with the LOD reaching 0.13 ng/mL (Figures 5 and S3).

Serum Sample Analysis. To demonstrate the potential application of our developed trypsin sensor for clinical sample analysis, one human serum (from human male AB plasma, USA origin, Sigma-Aldrich, St. Louis, MO) was examined. Briefly, the serum sample (1:20 dilution in PBS) was analyzed by our constructed sensor, and the trypsin concentration in the diluted sample was determined to be 6.5 ± 0.2 ng/mL, which is equivalent to ∼130 ng/mL in the original serum sample, and this value is within the serum trypsin concentration range of healthy population (ranging from 115 to 350 ng/mL). To further evaluate the effect of the matrix components on trypsin detection, three additional mock serum samples were analyzed, and these samples were prepared by spiking trypsin standard solutions with varying concentrations to the diluted (1:20) human serum. The results were summarized in Table 1. From the table, we could see that our developed CRISPR-based activity assay possessed satisfactory sensing performance toward trypsin detection, with recoveries obtained ranging from 105 to 129%. The experimental results suggest that our developed trypsin activity assay will not significantly be affected by the serum matrix, and offers a potential use as a noninvasive/minimally invasive tool in clinical diagnosis.

Table 1. Serum Sample Analysis Using the Developed CRISPR-Based Trypsin Activity Assay Platform

sample number	trypsin added (ng/mL)	trypsin found[a] (ng/mL)	trypsin recovered (ng/mL)	recovery (%)
1	0	6.5 ± 0.2	—	—
2	10	19.4 ± 1.3	12.9	129.0 ± 8.0
3	20	31.7 ± 1.0	25.2	126.0 ± 3.7
4	50	59.0 ± 2.7	52.5	105.0 ± 4.8

[a]Each value represents the mean of three replicate analyses ± one standard deviation.

CONCLUSION

In summary, by taking advantage of a magnetic bead-gold nanoparticle assembly, which carries the peptide substrate and tens to hundreds of DNA molecules per peptide molecule, coupled with CRISPR analysis, a highly sensitive and selective trypsin activity assay was developed. Although the entire investigation focused on trypsin, it can be visualized that the sensing strategy pioneered in this work may be utilized to develop sensors for a wide variety of proteases and enzymes. For this purpose, the magnetic beads-based sensing platform constructed in this study can be easily expanded by using a 96-well or 384-well streptavidin coated-polystyrene plate. By immobilizing a series of AuNPs dual-functionalized with barcode ssDNA and various selective peptide substrates for various proteases to the plate, a large-scale multiplexing tool for high-throughput detection of protease biomarkers could be fabricated. Moreover, it should be noted that, the trypsin sensor constructed in this work was not optimized. To further improve the LOD of the sensor, several factors need to be systematically investigated, including the peptide length, substrate cleavage site design as well as the length and sequence of the barcode DNA. Given the ultrahigh sensitivity, the CRISPR-based protease activity assay platform developed in this work offers the potential as a tool for disease diagnosis.

ASSOCIATED CONTENT

Supporting Information

The Supporting Information is available free of charge at https://pubs.acs.org/doi/10.1021/acsabm.5c00854.

(PDF)

AUTHOR INFORMATION

Corresponding Author

Xiyun Guan − *Department of Chemistry, University of Missouri, Columbia, Missouri 65211, United States;* orcid.org/0000-0003-2022-4872; Email: xgpc2@missouri.edu

Authors

Sathishkumar Munusamy − *Department of Chemistry, University of Missouri, Columbia, Missouri 65211, United States*

Haiyan Zheng − *Department of Chemistry, University of Missouri, Columbia, Missouri 65211, United States*

Jun Chen − *Department of Chemistry, University of Missouri, Columbia, Missouri 65211, United States*

Shuo Zhou − *Department of Chemistry, University of Missouri, Columbia, Missouri 65211, United States;* orcid.org/0000-0002-7491-3983

Juanhua Kong − *Department of Chemistry, University of Missouri, Columbia, Missouri 65211, United States*

Rana Jahani − *Department of Chemistry, University of Missouri, Columbia, Missouri 65211, United States*

Yuan Zhao − *Department of Chemistry, University of Missouri, Columbia, Missouri 65211, United States*

Complete contact information is available at: https://pubs.acs.org/10.1021/acsabm.5c00854

Author Contributions

Sathishkumar Munusamy: investigation, methodology, data curation, formal analysis, writing - original draft. Haiyan Zheng: data curation, formal analysis, investigation. Jun Chen: investigation. Shuo Zhou: investigation. Juanhua Kong: investigation. Rana Jahani: investigation. Yuan Zhao: investigation. Xiyun Guan: conceptualization, supervision, project administration, writing - review and editing.

Notes

The authors declare no competing financial interest.

ACKNOWLEDGMENTS

This work was financially supported by the National Institutes of Health (R01GM147247) and National Science Foundation (2203763 and 2345813).

REFERENCES

(1) Shah, H.; Fairlie, D. P.; Lim, J. Protease-Activated Receptor 2: A Promising Therapeutic Target for Women's Cancers. *J. Pharmacol. Exp. Ther.* **2025**, *392* (1), 100016.

(2) Sarode, G. S.; Sarode, S. C.; Ghone, U.; Anand, R. Role of Proteases in Oral Carcinogenesis: Insights into the Cancer Degradome and Therapeutic Implications. *Oral Oncol. Rep.* **2024**, *10*, 100542.

(3) Gordon, S. M.; Remaley, A. T. High Density Lipoproteins Are Modulators of Protease Activity: Implications in Inflammation, Complement Activation, and Atherothrombosis. *Atherosclerosis* **2017**, *259*, 104−113.

(4) Weidmann, H.; Heikaus, L.; Long, A. T.; Naudin, C.; Schlüter, H.; Renné, T. The Plasma Contact System, a Protease Cascade at the Nexus of Inflammation, Coagulation and Immunity. *Biochim. Biophys. Acta, Mol. Cell Res.* **2017**, *1864* (11), 2118−2127.

(5) Yamashita, K.; Mimori, K.; Inoue, H.; Mori, M.; Sidransky, D. A Tumor-Suppressive Role for Trypsin in Human Cancer Progression. *Cancer Res.* **2003**, *63* (20), 6575−6578.

(6) Hirota, M.; Ohmuraya, M.; Baba, H. The Role of Trypsin, Trypsin Inhibitor, and Trypsin Receptor in the Onset and Aggravation of Pancreatitis. *J. Gastroenterol.* **2006**, *41* (9), 832−836.

(7) Chen, N.; Zou, J.; Wang, S.; Ye, Y.; Huang, Y.; Gadda, G.; Yang, J. J. Designing Protease Sensors for Real-Time Imaging of Trypsin Activation in Pancreatic Cancer Cells. *Biochemistry* **2009**, *48* (15), 3519−3526.

(8) Scott, J. I.; Deng, Q.; Vendrell, M. Near-Infrared Fluorescent Probes for the Detection of Cancer-Associated Proteases. *ACS Chem. Biol.* **2021**, *16* (8), 1304−1317.

(9) Giel, M.-C.; Zhang, S.; Hu, Q.; Ding, D.; Tang, Y.; Hong, Y. Synthesis of a β-Arylethenesulfonyl Fluoride-Functionalized AIEgen for Activity-Based Urinary Trypsin Detection. *ACS Appl. Bio Mater.* **2022**, *5* (9), 4321−4326.

(10) Park, T.; Han, M.; Schanze, K. S.; Lee, S. H. Ultrasensitive Determination of Trypsin in Human Urine Based on Amplified Fluorescence Response. *ACS Sensors* **2023**, *8* (7), 2591−2597.

(11) Vandermarliere, E.; Mueller, M.; Martens, L. Getting Intimate with Trypsin, the Leading Protease in Proteomics. *Mass Spectrom. Rev.* **2013**, *32* (6), 453−465.

(12) Seia, M. A.; Stege, P. W.; Pereira, S. V.; De Vito, I. E.; Raba, J.; Messina, G. A. Silica Nanoparticle-Based Microfluidic Immunosensor with Laser-Induced Fluorescence Detection for the Quantification of Immunoreactive Trypsin. *Anal. Biochem.* **2014**, *463*, 31−37.

(13) Lefkowitz, R. B.; Schmid-Schönbein, G. W.; Heller, M. J. Whole Blood Assay for Trypsin Activity Using Polyanionic Focusing Gel Electrophoresis. *Electrophoresis* **2010**, *31* (14), 2442−2451.

(14) Shin, J.; Park, K.; Park, S.; Yang, H. Trypsin Detection Using Electrochemical Reduction-Based Redox Cycling. *Bull. Korean Chem. Soc.* **2021**, *42* (1), 37−42.

(15) Shantiaei, H.; Roushani, M.; Mohammadi, F. Electrospinning ZnS:Ni Quantum Dots into Carbon Nanofibrous Structure as a Base for the Electrochemical Aptasensor for Detection of Trypsin. *Sens. Actuators Rep.* **2025**, *9*, 100272.

(16) Wang, J.; Kong, J.; Zhang, X. Riboflavin-Induced Photo-ATRP Electrochemical Strategy for Detection of Biomarker Trypsin. *Talanta* **2024**, *277*, 126386.

(17) Hu, J.; Li, Q.; Chen, J.; Chen, S.; Cai, Y.; Zhao, C. A Label-Free Electrochemical Immunosensor Based on Polythionine-Nanogold Nanocomposite for Detection of Trypsin Using Screen-Printed Electrode. *Int. J. Electrochem. Sci.* **2022**, *17* (6), 220617.

(18) You, X.; Li, Y.; Li, B.; Ma, J. Gold Nanoclusters-Based Chemiluminescence Resonance Energy Transfer Method for Sensitive and Label-Free Detection of Trypsin. *Talanta* **2016**, *147*, 63−68.

(19) Zhou, S.; Wang, L.; Chen, X.; Guan, X. Label-Free Nanopore Single-Molecule Measurement of Trypsin Activity. *ACS Sensors* **2016**, *1* (5), 607−613.

(20) Luo, Q.; Tian, M.; Luo, F.; Zhao, M.; Lin, C.; Qiu, B.; Wang, J.; Lin, Z. Multicolor Biosensor for Trypsin Detection Based on the Regulation of the Peroxidase Activity of Bovine Serum Albumin-Coated Gold Nanoclusters and Etching of Gold Nanobipyramids. *Anal. Chem.* **2023**, *95* (4), 2390−2397.

(21) Tan, Q.; Zhang, R.; Kong, W.; Qu, F.; Lu, L. Ascorbic Acid-Loaded Apoferritin-Assisted Carbon Dot-MnO2 Nanocomposites for the Selective and Sensitive Detection of Trypsin. *ACS Appl. Bio Mater.* **2018**, *1* (3), 777−782.

(22) Upadhaya, A. H.; Mirgane, H. A.; Pandey, S. P.; Patil, V. S.; Bhosale, S. V.; Singh, P. K. Electrostatically Engineered Tetraphenylethylene-Based Fluorescence Sensor for Protamine and Trypsin: Leveraging Aggregation-Induced Emission for Enhanced Sensitivity and Selectivity. *Langmuir* **2024**, *40* (37), 19357−19369.

(23) Seo, S.; Kim, J.; Jang, G.; Kim, D.; Lee, T. S. Aggregation−Deaggregation-Triggered, Tunable Fluorescence of an Assay Ensemble Composed of Anionic Conjugated Polymer and Polypeptides by Enzymatic Catalysis of Trypsin. *ACS Appl. Mater. Interfaces* **2014**, *6* (2), 918−924.

(24) Zhao, L.; Wang, T.; Wu, Q.; Liu, Y.; Chen, Z.; Li, X. Fluorescent Strips of Electrospun Fibers for Ratiometric Sensing of Serum Heparin and Urine Trypsin. *ACS Appl. Mater. Interfaces* **2017**, *9* (4), 3400−3410.

(25) Lai, Z.; Wang, F.; Cui, Y.; Li, Z.; Lin, J. Innovative Strategies for Enhancing AuNP-Based Point-of-Care Diagnostics: Focus on Coronavirus Detection. *Talanta* **2025**, *285*, 127362.

(26) Siciliano, G.; Alsadig, A.; Chiriacò, M. S.; Turco, A.; Foscarini, A.; Ferrara, F.; Gigli, G.; Primiceri, E. Beyond Traditional Biosensors: Recent Advances in Gold Nanoparticles Modified Electrodes for Biosensing Applications. *Talanta* **2024**, *268*, 125280.

(27) Eivazzadeh-Keihan, R.; Saadatidizaji, Z.; Mahdavi, M.; Maleki, A.; Irani, M.; Zare, I. Recent Advances in Gold Nanoparticles-Based Biosensors for Tuberculosis Determination. *Talanta* **2024**, *275*, 126099.

(28) Vairaperumal, T.; Huang, C.-C.; Liu, P.-Y. Optical Nanobiosensor-Based Point-of-Care Testing for Cardiovascular Disease Biomarkers. *ACS Appl. Bio Mater.* **2023**, *6* (7), 2591−2613.

(29) Zare, I.; Yaraki, M. T.; Speranza, G.; Najafabadi, A. H.; Shourangiz-Haghighi, A.; Nik, A. B.; Manshian, B. B.; Saraiva, C.; Soenen, S. J.; Kogan, M. J.; Lee, J. W.; Apollo, N. V.; Bernardino, L.; Araya, E.; Mayer, D.; Mao, G.; Hamblin, M. R. Gold Nanostructures: Synthesis, Properties, and Neurological Applications. *Chem. Soc. Rev.* **2022**, *51* (7), 2601−2680.

(30) Türkmen, D.; Bakhshpour, M.; Göktürk, I.; Aşır, S.; Yılmaz, F.; Denizli, A. Selective Dopamine Detection by SPR Sensor Signal Amplification Using Gold Nanoparticles. *New J. Chem.* **2021**, *45* (39), 18296−18306.

(31) Sarfraz, N.; Khan, I. Plasmonic Gold Nanoparticles (AuNPs): Properties, Synthesis and Their Advanced Energy, Environmental and Biomedical Applications. *Chem. Asian J.* **2021**, *16* (7), 720−742.

(32) Tang, Y.; Mo, X.; Yuan, L.; Huang, X.; Yan, Y.; Jin, W.; Zhang, L.; Jiang, X.; Nie, J.; Zhang, Y. Tyndall-Effect-Amplified Colorimetric Detection of Trypsin Based on the Analyte-Regulated Formation of Au Nanoparticle Network with No Visual Change in Surface Plasmon Resonance Response. *Sens. Actuators B* **2024**, *405*, 135254.

(33) Zhou, Z.; Liu, W.; Wang, Y.; Ding, F.; Liu, X.; Zhao, Q.; Zou, P.; Wang, X.; Rao, H. A Fluorometric and Colorimetric Method for Determination of Trypsin by Exploiting the Gold Nanocluster-Induced Aggregation of Hemoglobin-Coated Gold Nanoparticles. *Microchim. Acta* **2019**, *186* (5), 272.

(34) Xu, S.; Zhang, F.; Xu, L.; Liu, X.; Ma, P.; Sun, Y.; Wang, X.; Song, D. A Fluorescence Resonance Energy Transfer Biosensor Based on Carbon Dots and Gold Nanoparticles for the Detection of Trypsin. *Sens. Actuators B* **2018**, *273*, 1015−1021.

(35) Wang, M.; Su, D.; Wang, G.; Su, X. A Fluorometric Sensing Method for Sensitive Detection of Trypsin and Its Inhibitor Based on Gold Nanoclusters and Gold Nanoparticles. *Anal. Bioanal. Chem.* **2018**, *410* (26), 6891−6900.

(36) Creyer, M. N.; Jin, Z.; Moore, C.; Yim, W.; Zhou, J.; Jokerst, J. V. Modulation of Gold Nanorod Growth via the Proteolysis of Dithiol Peptides for Enzymatic Biomarker Detection. *ACS Appl. Mater. Interfaces* **2021**, *13* (38), 45236−45243.

https://doi.org/10.1021/acsabm.5c00854
ACS Appl. Bio Mater. XXXX, XXX, XXX−XXX

(37) Wang, S.; Shen, X.; Chen, G.; Zhang, W.; Tan, B. Application and Development of CRISPR-Cas12a Methods for the Molecular Diagnosis of Cancer: A Review. *Anal. Chim. Acta* **2025**, *1341*, 343603.
(38) Lv, Z.; Wang, Q.; Yang, M. Multivalent Duplexed-Aptamer Networks Regulated a CRISPR-Cas12a System for Circulating Tumor Cell Detection. *Anal. Chem.* **2021**, *93* (38), 12921−12929.
(39) Xiong, Y.; Zhang, J.; Yang, Z.; Mou, Q.; Ma, Y.; Xiong, Y.; Lu, Y. Functional DNA Regulated CRISPR-Cas12a Sensors for Point-of-Care Diagnostics of Non-Nucleic-Acid Targets. *J. Am. Chem. Soc.* **2020**, *142* (1), 207−213.
(40) Ci, Q.; He, Y.; Chen, J. Novel Anti-CRISPR-Assisted CRISPR Biosensor for Exclusive Detection of Single-Stranded DNA (ssDNA). *ACS Sensors* **2024**, *9* (3), 1162−1167.
(41) Munusamy, S.; Zheng, H.; Jahani, R.; Zhou, S.; Chen, J.; Kong, J.; Guan, X. DNA-Assisted CRISPR-Cas12a Enhanced Fluorescent Assay for Protein Detection in Complicated Matrices. *ACS Appl. Bio Mater.* **2025**, *8* (1), 754−762.
(42) Munusamy, S.; Zheng, H.; Jahani, R.; Zhou, S.; Chen, J.; Kong, J.; Guan, X. Enzyme-Free Immunoassay for Rapid, Sensitive, and Selective Detection of C-Reactive Protein. *Anal. Bioanal. Chem.* **2024**, *416* (29), 6985−6994.
(43) Zhang, Y.; Chen, X.; Wang, C.; Chang, H.-C.; Guan, X. Nanoparticle-Assisted Detection of Nucleic Acids in a Polymeric Nanopore with a Large Pore Size. *Biosens. Bioelectron.* **2022**, *196*, 113697.
(44) Zhang, Y.; Chen, X.; Wang, C.; Roozbahani, G. M.; Chang, H.-C.; Guan, X. Chemically Functionalized Conical PET Nanopore for Protein Detection at the Single-Molecule Level. *Biosens. Bioelectron.* **2020**, *165*, 112289.
(45) Arora, P.; Zheng, H.; Munusamy, S.; Jahani, R.; Guan, X. Nanopore-Based Detection of Periodontitis Biomarker miR31 in Saliva Samples. *Electrophoresis* **2024**, *45* (21−22), 2034−2044.
(46) Zheng, H.; Munusamy, S.; Zhou, S.; Jahani, R.; Chen, J.; Kong, J.; Guan, X. Nanopore Detection of Small Molecules Based on Replacement and Complexation Chemical Interactions. *Small* **2025**, *21* (15), 2407184.
(47) Zheng, H.; Munusamy, S.; Arora, P.; Jahani, R.; Guan, X. A Highly Sensitive Nanopore Platform for Measuring RNase A Activity. *Talanta* **2024**, *276*, 126276.
(48) Chen, X.; Zhou, S.; Wang, Y.; Zheng, L.; Guan, S.; Wang, D.; Wang, L.; Guan, X. Nanopore Single-Molecule Analysis of Biomarkers: Providing Possible Clues to Disease Diagnosis. *TrAC, Trends Anal. Chem.* **2023**, *162*, 117060.
(49) Reitemeier, J.; Metro, J.; Fu, K. X. Nanopore Sensing and beyond: Electrochemical Systems for Optically-Coupled Single-Entity Studies, Stimulus-Responsive Gating Applications, and Point-of-Care Sensors. *Sens. Actuators Rep.* **2024**, *8*, 100225.
(50) Jia, J.; Kwon, S.-R.; Baek, S.; Sundaresan, V.; Cao, T.; Cutri, A. R.; Fu, K.; Roberts, B.; Shrout, J. D.; Bohn, P. W. Actively Controllable Solid-Phase Microextraction in a Hierarchically Organized Block Copolymer-Nanopore Electrode Array Sensor for Charge-Selective Detection of Bacterial Metabolites. *Anal. Chem.* **2021**, *93* (43), 14481−14488.
(51) Wang, L.; Zhou, S.; Wang, Y.; Wang, Y.; Li, J.; Chen, X.; Zhou, D.; Liang, L.; Yin, B.; Zhang, Y.; Wang, L. Molecular Sandwich-based DNAzyme Catalytic Reaction towards Transducing Efficient Nanopore Electrical Detection of Antigen Proteins. *Faraday Discuss.* **2025**, *257*, 60−72.
(52) Chen, X. M.; M Roozbahani, G.; Ye, Z.; Zhang, Y.; Ma, R.; Xiang, J.; Guan, X. Label-Free Detection of DNA Mutations by Nanopore Analysis. *ACS Appl. Mater. Interfaces* **2018**, *10* (14), 11519−11528.
(53) Liu, Q.; Ouyang, Y.; Wang, Y.; Zhou, S.; Zhan, Y.; Wang, L. Multianalyte Nanopore Detection of Alzheimer's Disease Biomarkers: A Label-Free Platform with Improved Sensitivity and Range. *Adv. Healthcare Mater.* **2025**, 2405058.
(54) Roozbahani, G. M.; Zhang, Y.; Chen, X.; Soflaee, M. H.; Guan, X. Enzymatic- Reaction based nanopore Detection of Zinc Ions. *Analyst* **2019**, *144*, 7432−7436.
(55) Chan, C. W.-T.; Cheng, H.-K.; Hau, F. K.-W.; Chan, A. K.-W.; Yam, V. W.-W. Protamine-Induced Supramolecular Self-Assembly of Red-Emissive Alkynylplatinum(II) 2,6-Bis(Benzimidazol-2′-Yl)-Pyridine Complex for Selective Label-Free Sensing of Heparin and Real-Time Monitoring of Trypsin Activity. *ACS Appl. Mater. Interfaces* **2019**, *11* (35), 31585−31593.
(56) Gao, P.; Wu, S.; Chang, X.; Liu, F.; Zhang, T.; Wang, B.; Zhang, K.-Q. Aprotinin Encapsulated Gold Nanoclusters: A Fluorescent Bioprobe with Dynamic Nuclear Targeting and Selective Detection of Trypsin and Heavy Metal. *Bioconjugate Chem.* **2018**, *29* (12), 4140−4148.
(57) Nguyen, L. T.; Smith, B. M.; Jain, P. K. Enhancement of Trans-Cleavage Activity of Cas12a with Engineered crRNA Enables Amplified Nucleic Acid Detection. *Nat. Commun.* **2020**, *11* (1), 4906.

https://doi.org/10.1021/acsabm.5c00854
ACS Appl. Bio Mater. XXXX, XXX, XXX−XXX